Subsuns, Bottlinger's rings, and elliptical halos

David K. Lynch, Stanley D. Gedzelman, and Alistair B. Fraser

Subsuns, Bottlinger's rings, and elliptical halos are simulated by the use of a Monte Carlo model; reflection of sunlight from almost horizontal ice crystals is assumed. Subsuns are circular or elliptical spots seen at the specular reflection point when one flies over cirrus or cirrostratus clouds. Bottlinger's rings are rare, almost elliptical rings centered about the subsun. Elliptical halos are small rings of light centered around the Sun or the Moon that rarely occur with other halo phenomena. Subsuns and Bottlinger's rings can be explained by reflection from a single crystal, whereas elliptical halos require reflection from two separate crystals. All three phenomena are colorless and vertically elongated with an eccentricity that increases with increasing solar zenith angle. For several cases of Bottlinger's rings the simulations are compared with density scans of photographs. Clouds that consist of large swinging or gyrating plates and dendritic crystals, which form near −15 °C, seem the most likely candidates to produce the rings and elliptical halos. Meteorological evidence is presented that supports these conditions for elliptical halos. Simulations suggest that the most distinct elliptical halos may be produced by hybrid clouds that contain both horizontal and gyrating crystals.

Introduction

Subsuns are among the brightest atmospheric optical phenomena produced by hydrometeors, but they were not described until after a balloon ascent in 1840.[1] Flight has now made sightings of subsuns relatively common, for they are produced by the reflection of sunlight from almost horizontally oriented ice crystals and appear at the specular (subsolar) point, directly below the Sun and as far below the horizon as the Sun is above it. Many subsuns are approximately elliptical and, when so, are always elongated in the vertical plane. Elliptical subsuns are caused by reflection from ice crystals that tilt slightly.

Little theoretical work has been done on subsuns, probably because their origin seems obvious.[2,3] Simulations of pillars below the Sun,[4] which are equivalent to subsuns, have been limited to small solar altitudes. Subsun simulations by a phenomenological model that does not explicitly consider oriented ice crystals but rather relies on a plausible scattering function for a rough surface have been used in scene generation models.[5]

On rare occasions, the subsun is surrounded by an elliptical disk or ring. The phenomenon is named Bottlinger's rings after C. F. Bottlinger, who first reported seeing a hollow white elliptical ring surrounding a subsun during a balloon flight above a cloud consisting of "ice-needles" on 13 March 1909.[6] Bottlinger noted that the ring was 3°–4° in vertical extent and roughly 1.65 times higher than wide when the Sun was 37° above the horizon. The phenomenon lasted for over an hour, with the ring fading before the subsun.

Bottlinger invoked swinging crystals to explain the simultaneous presence of the ring and the subsun. He reasoned that the crystals spend most time near the maximum tilt, which accounts for the ring, whereas, when the ice crystals are horizontal, all the reflected light is focused at the subsolar point, which accounts for the subsun. Stuchtey then determined the precise shape of the rings.[7]

We know of only five photographs of Bottlinger's rings.[8,9] Three of these appear in Plates 26–29. The disparity between the frequently observed subsun and the rare sightings of Bottlinger's rings formed one of the initial motivations for this paper.

An even rarer atmospheric optical phenomenon is the elliptical halo. There were a few observations of elliptical halos early this century,[10–12] but the only known photographs and most of the observations have been made since 1987 by members of the

D. K. Lynch is with Thule Scientific, 22914 Portage Circle Drive, Topanga, California 90290; S. D. Gedzelman is with the Department of Earth and Atmospheric Sciences, City College of New York, New York, New York 10031; and A. B. Fraser is with the Department of Meteorology, The Pennsylvania State University, University Park, Pennsylvania 16802.

Received 1 December 1993; revised manuscript received 9 March 1994.

0003-6935/94/214580-10$06.00/0.

Finnish Halo Observing Network.[13–15] All elliptical halos are centered on the Sun or the Moon and are vertically elongated. Four of these are shown in the color plate section.[16] Of the 16 cases reported by the Finnish Network, 14 were colorless and two (not photographed) had a slight red color on the inside. It is on the basis of their lack of color that they are distinguished from elliptical coronas.[17] Most elliptical halos appear to be hallow rings although three solid disks were reported. Most elliptical halos have a vertical diameter of at least 6°. Smaller elliptical halos and disks would tend not to be observed because they are easily overwhelmed by scattered light of the Sun's aureole.

Perhaps the most intriguing observation is that elliptical halos occur alone and are formed in a different cloud type than common halos. When other halos have been observed at the same time, they appear to be produced in clouds at a different level. One exception occurred on 12 April 1993, when three concentric elliptical halos were reported as part of a complex halo display.

We propose here that most elliptical halos, like Bottlinger's rings, are produced by reflection of light from nearly horizontal crystals. However, in order for a reflection halo to form around the Sun or the Moon, the light must be reflected by two separate ice crystals. Several issues must therefore be addressed in any theory of elliptical halos. First, simulations must show the proper spatial distribution of intensities. Second, few halo phenomena have undisputably been attributed to multiple reflections, and it is not obvious that any halo so produced would be bright enough to be seen. Finally, simulations by horizontal plate crystals of finite thickness invariably include halo phenomena such as parhelia, whereas most elliptical halos are seen without any refraction halos.

The theory for subsuns, Bottlinger's rings, and elliptical halos presented here therefore takes into account not only the geometric optics of reflection from tilted crystals, but the likely shapes, sizes, and fall modes of the crystals involved, as well as the effects of radiative transfer of light through clouds of finite optical thickness.

We begin by presenting the results of scanned photographs of Bottlinger's rings. We then consider the reflection geometry and the expected shape of the rings. Observations of crystal fall modes are briefly reviewed. We then present the simulations for different crystal tilt populations. Finally, we treat the impact of clouds with finite optical thickness on the brightness of the elliptical halos.

Density Scans of Bottlinger's Rings

By the use of a densitometer, horizontal and vertical density scans were taken through the center of four photographs of Bottlinger's rings (Figs. 1–4). The photographs were not intensity calibrated, but their brightness properties should be qualitatively correct, as the mapping from density to intensity is unique and monotonic. Peak intensities will not be well represented if the film has been overexposed.

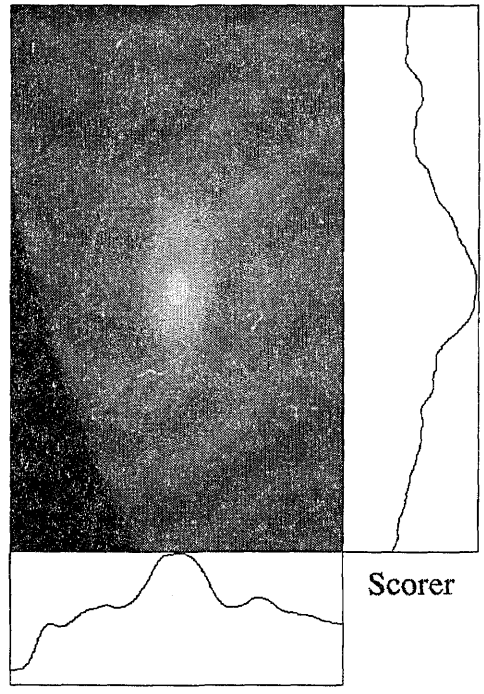

Fig. 1. Density scans through subsun and Bottlinger's ring that appear as Plate 13.3.11 in Ref. 8.

In most cases the density scans tell a somewhat different story than the eye. Looking across the equatorial plane of Plate 26 and Fig. 2 suggests that there are three distinct concentric bands. The scan does show the maximum, but then shows a monotonic decrease of intensity with only a small hump corresponding to the second band. The vertical scan reveals a marked asymmetry, with brighter values at the top, or near the horizon. This asymmetry results from the increase of both the effective optical thickness and the reflection coefficient as the horizon is approached. To the eye, both Plate 27 and Fig. 3 seem to have a distinct bright ring, but the density scan in the equatorial plane suggests that the bright ring is merely a region of more gradually decreasing intensity.

In short, the density scans show that the perceived brightness minima between the subsun and Bottlinger's ring are either absent or not as deep as perceived. This is an illusion related to the well-known Mach bands.[18,19] In fact, Bottlinger's rings are usually disks with a bright center and perhaps a slightly brighter fringe. A model of Bottlinger's rings should conform closely to the scanned intensity profiles.

Reflection Geometry

We assume that specular reflection from almost horizontal ice crystals produces subsuns, Bottlinger's rings, and elliptical halos. All three phenomena should then have basically the same shape, which depends largely on solar elevation angle and, to a lesser extent, on tilt angle.[7,20]

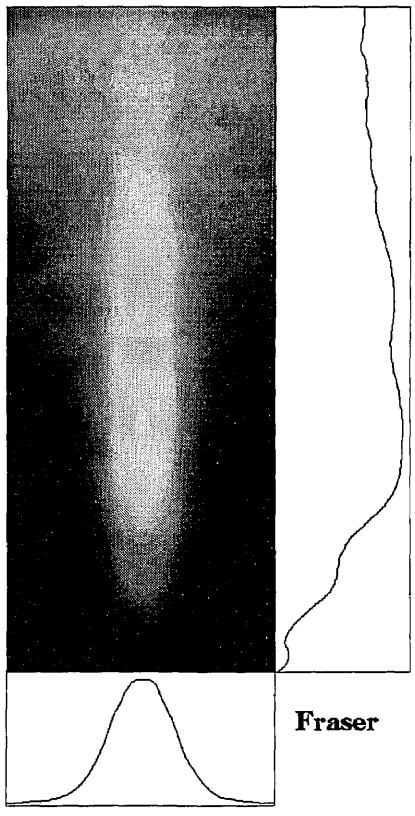

Fig. 2. Density scans through the subsun and Bottlinger's ring shown in Plate 26.

Fig. 3. Density scans through the subsun and Bottlinger's ring shown in Plate 27.

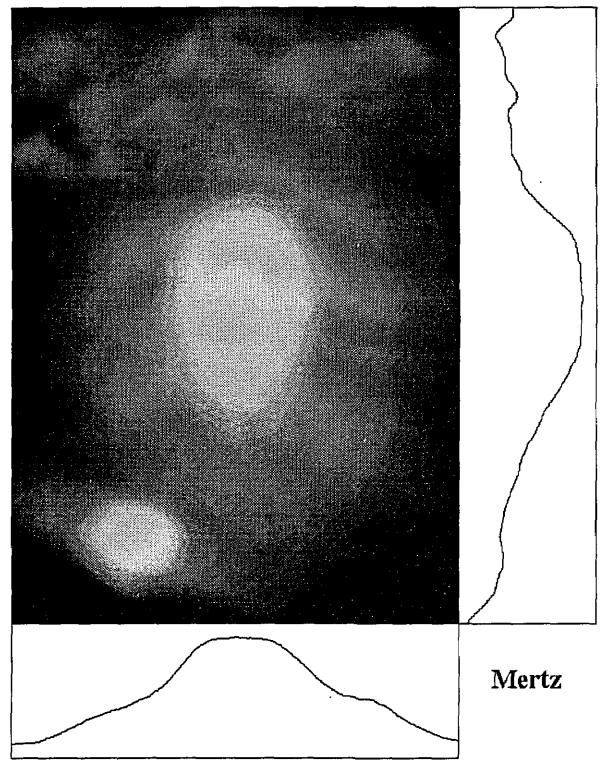

Fig. 4. Density scans through the subsun and Bottlinger's ring shown in Plate 28.

A simple vector solution of specular reflection from an arbitrarily oriented surface is used to solve the reflection geometry (Appendix A). Figure 5 shows their shapes for a point Sun with an altitude of 20° and several different values of tilt angle ψ. The rings are almond shaped rather than strictly elliptical. The asymmetry varies with crystal tip angle and is larger for small solar elevations.

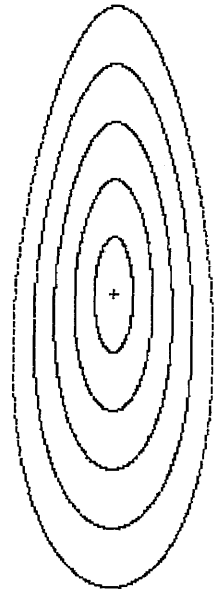

Fig. 5. Shape of the subsun and Bottlinger's ring for a solar elevation of 20° and maximum tilt angles of 1°, 2°, 3°, 4°, and 5°.

Figure 6 shows the effect of solar elevation on the shape of the rings for a constant tip angle. For a point Sun, the height of the ring is $4\psi_{max}$, whereas the width is approximately $4\psi_{max}\cos(\phi)$, where ψ_{max} is the maximum tilt of the crystals, and ϕ is the solar zenith angle. Thus, for a point Sun and small ψ, the ratio of width to height equals $\cos(\phi)$. In Plate 26, $\phi \approx 12°$ so that $\cos(12°) = 0.208$. This matches the observed width-to-height ratio almost exactly. Bottlinger's observation also matches the theoretical width-to-height ratio closely. For the elliptical halos, Fig. 7 shows that the ratio does increase with solar altitude, but that substantial discrepancies exist between theory and observation.

Fall Modes of Ice Crystals

Small plate crystals tend to fall horizontally and thus would produce only circular subsuns. As crystal size and Reynolds number R increase, eddies form in the wake of the falling crystals. For Reynolds numbers above $\sim R \approx 100$, eddy shedding initiates pendulum motion in which crystal tilt oscillates more or less sinusoidally (Fig. 8) with increasing maximum tilt for larger R.[21–24] For plate crystals, this occurs once the length exceeds ~ 1.5 mm,[25,26] although the swinging mode may be initiated for somewhat smaller asymmetric crystals. The tilt of swinging plates can be idealized by the equation

$$\psi = \psi_{max} \sin(\omega t),$$

although the crystals can oscillate about more than a single axis and therefore may not oscillate about 0 tilt. At $R \gg 100$, crystals may fall in a gyrating helical mode with a constant or nearly constant inclination (Fig. 9).[27] Such gyrating crystals should be at least several millimeters across and would not be very common.

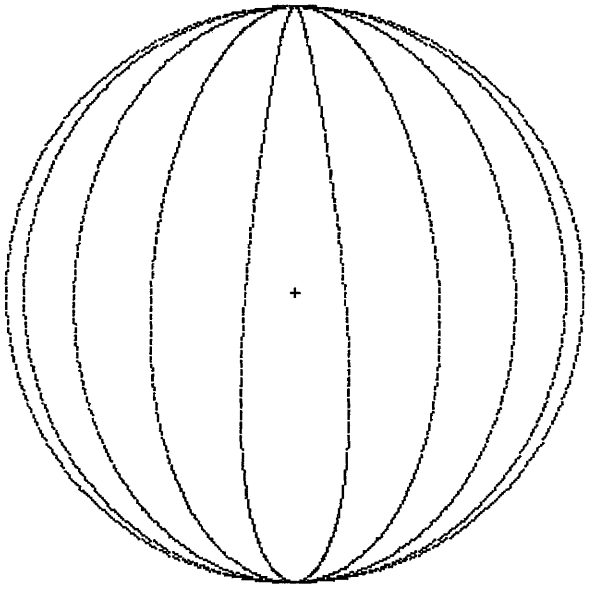

Fig. 6. Shape of the subsun and Bottlinger's ring for a maximum tilt of 2° and for solar elevations of 10°, 30°, 50°, 70°, and 90°.

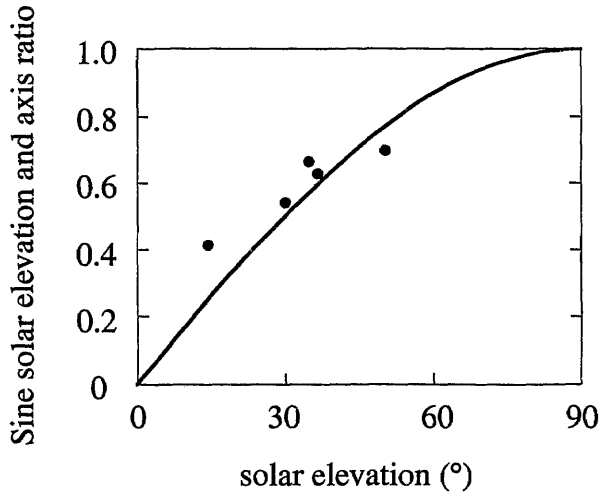

Fig. 7. Comparison of observations and theory of the width-to-height ratio of elliptical halos as a function of solar zenith angle.

Thus any halo phenomenon caused by tilted crystals must be produced by clouds that include substantial numbers of rather large crystals. This is not likely to occur often and may account for the rarity of Bottlinger's rings and elliptical halos. Only stellar and dendritic crystals, which form at temperatures near −15 °C and large supersaturations readily grow to such large sizes.[28] Interestingly, such multifaceted crystals cannot produce coherent refraction halos, a fact consistent with the observation that elliptical halos are seldom if ever associated with other halo phenomena.

Meteorological evidence supports the idea that elliptical halos form in clouds at approximately −15 °C and therefore probably consist of dendrites and stellars. Data near Vaasa, Finland, were obtained from constant pressure charts and surface weather maps at or around the times of three of the occurrences (00 UTC 8 December 1987, 12 UTC 18 February 1988, and 00 UTC 24 April 1988), whereas only the surface map was obtained for a fourth occurrence (12 April 1993). All reveal surprising similarities. In each

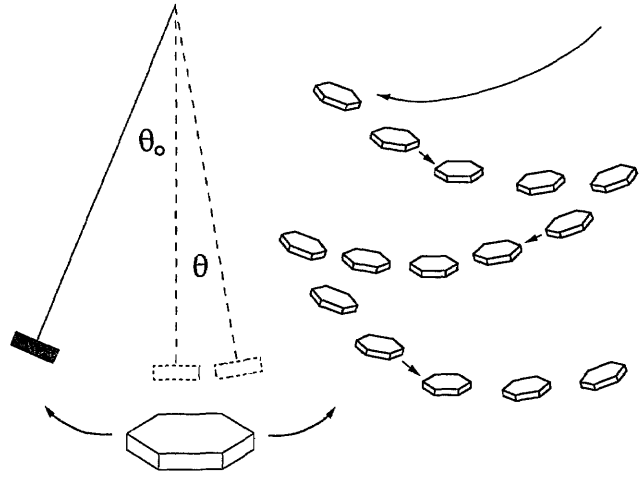

Fig. 8. Pendulum motion of a plate crystal.

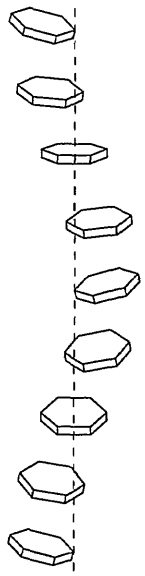

Fig. 9. Gyrational motion of a plate crystal.

case, an occluded low-pressure area was centered just southeast of Finland. The most humid standard layer was 850 mb, in which the temperature was either −14 or −15 °C and dew-point depressions were 5 °C or less. By contrast, drier air with dew-point depressions of at least 10 °C at or above 500 mb made high-level cirrostratus unlikely in each case.

Simulations

As most clouds consist of a spectrum of different size particles, they may also contain crystals with several different fall modes. Direct optical evidence for such rogue crystals is provided by the bright spots of light from diamond dust surrounding the elliptical subsun in a photograph by Tape (Plates 3–9 of Ref. 12). In the simulations below we therefore consider clouds that consist of crystals with either one or two different fall modes.

The simulations were designed to determine the conditions that are needed to duplicate the observed geometry and intensity patterns of the phenomena. We use a Monte Carlo approach[29] in which sunbeams strike one or two crystals with randomly assigned azimuth angle and tilt angles distributed according to the preselected fall mode. For simulations of Bottlinger's rings, the light strikes only single crystals, whereas the simulations of elliptical halos required that light beams be reflected by two separate crystals. In the runs in which only the shape or the spatial distribution of light in the rings is important, each light beam striking a crystal is reflected. In the runs designed to compare the intensity of the phenomena for different solar zenith angles and crystal shapes, the Fresnel reflection coefficients and the crystal aspect ratio (ratio of length to height) are included. In most simulations the finite width of the Sun (0.5°) is included because the phenomena extend over relatively small angles. The finite Sun maps all rings and spots produced by a point Sun over the area of the solar disk and smears the phenomena.

Figure 10 shows the dependence of Bottlinger's rings on the tilt distribution by comparing the intensity pattern of reflected light for harmonically swinging crystals with that for a uniform distribution of tilts when $\phi = 70°$ and $\psi_{max} = 2°$. Both cases produce well-defined elliptical subsuns, but in all other respects the patterns are quite different. For simple harmonic pendulum motion, the crystals spend a larger time near maximum tilt. This leads to a brighter periphery than for the pattern produced by crystals that spend an equal time at all tilts. The harmonically swinging crystals produce the illusion of a ring outside the subsun, even though the density of dots is almost uniform to the periphery. The cloud with a uniform distribution of tilts produces a disk with a faint periphery that neither gives the illusion of a ring nor matches the observations well. The uniform distribution of tilts may be used to represent a cloud in which the crystals have a wide range of maximum tilts and therefore a cloud that does not produce Bottlinger's rings.

Bottlinger's reasoning explains the simultaneous presence of the subsun and the disk ring. For a point Sun, the intensity of light in any ellipse is inversely proportional to the perimeter and directly proportional to the number of crystals or the time spent by a given crystal at the particular tilt. As a result, a horizontal scan of intensity through the equational plane of the Bottlinger ring for a point Sun and swinging crystals is proportional to

$$I(\psi) \propto \psi \frac{1}{\left[1 - \left(\frac{\psi}{\psi_{max}}\right)^2\right]^{1/2}}.$$

This expression has one maximum at $\psi = 0$ and one at

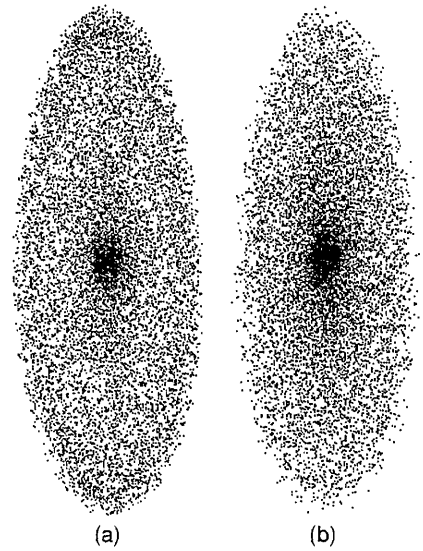

Fig. 10. Simulation for (a) harmonic tilt distribution and (b) uniform tilt distribution for solar zenith angle $\phi = 70°$ and maximum tilt $\psi_{max} = 2°$. Note that only (a) produces a Bottlinger's ring.

$\psi = \psi_{max}$ (Fig. 11). The maximum at $\psi = 0$, which leads to the subsun, is pronounced and, for crystal tilts of the order of 1° and low Sun altitudes, has an angular width close to that of the Sun. It remains pronounced when the finite size of the Sun is included and always produces a bright subsun. The maximum at $\psi = \psi_{max}$, which leads to the ring, is so narrow that it is either severely reduced or eliminated by the Sun's finite size. As a result, a distinct ring surrounding dark sky is not common. Furthermore, because swinging crystals in a cloud have different maximum tilts except under the most uniform conditions, the intensity maximum seldom occurs at the outer edge of Bottlinger's ring.

The maximum value of crystal tilt also determines whether a distinct ring is possible. Figure 12 shows the brightness distributions for pendulum motion with maximum tilts of 4°, 2°, and 1°. In all cases, the subsun is approximately as wide as the sun, but the ring width increases with crystal tilt and separates from the subsun only for $\psi_{max} > 1°$. Similarly, increasing the solar elevation angle has a greater effect on the size of the ring than on the size of the spot so that a distinct ring is more likely to be seen for a higher Sun.

Only gyrating crystals can produce a distinct Bottlinger ring surrounding a dark sky. Nevertheless, a cloud that consists solely of gyrating crystals cannot produce the subsun that has always been observed with the ring (Fig. 13). Therefore, if gyrating crystals do produce a ring, then the cloud must also contain either swinging or horizontal crystals. The assumption that clouds contain crystals with different fall modes (or several different crystal types) has been invoked in simulations of halo complexes.[14]

Clouds that possess several different crystal fall modes may also produce elliptical halos, as any small reflection halo surrounding the Sun or the Moon requires reflection from a second nearly horizontal ice crystal to redirect the light downward. In our simulations of elliptical halos, we considered the effect of all possible combinations of horizontal, swinging, and gyrating crystals on the resulting halo form. Simulations of three different tilt cases are shown in Fig. 14, and their horizontal intensity profiles are shown in Fig. 15. Clouds that consist entirely of swinging crystals produce aureoles that fade rapidly outward rather than distinct elliptical halos or disks. Clouds that consist entirely of crystals that gyrate at the same tilt produce both a bright virtual Sun and a discernible but not pronounced ring surrounding a disk. The first reflection from gyrating crystals creates a distinct (Bottlinger) ring, whereas the second reflection from gyrating crystals redirects the light downward while mapping a new ring around each portion of the first ring. This smudges the pattern and leads to a disk with a somewhat brighter periphery and a vertical angular diameter eight times the crystal tilt.

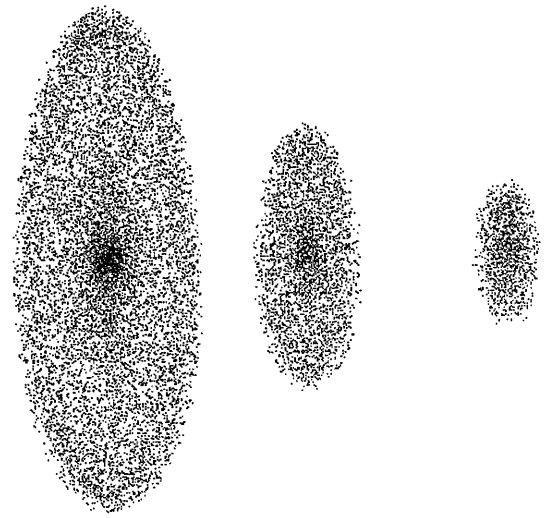

Fig. 12. Simulation of subsuns and Bottlinger's rings for swinging crystals with pendulum distributions for ψ_{max} equal to 4°, 2°, and 1°. Note that all subsuns are approximately the same size and that the Bottlinger rings disappear for small maximum tilts.

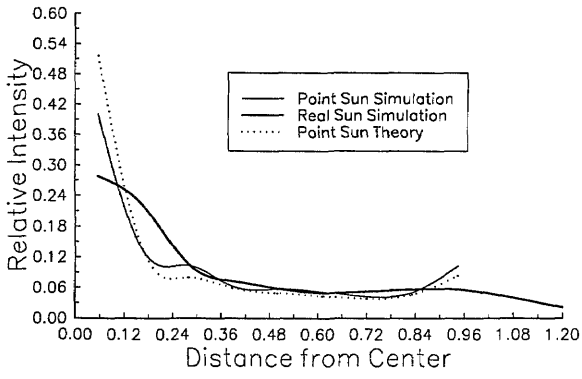

Fig. 11. Effect of the finite size of the Sun on the simulated and the threoretical relative intensity profiles in the horizontal plane of the subsun and Bottlinger's ring for a cloud of swinging crystals for $\phi = 70°$ and $\psi_{max} = 1.5°$. A maximum at the outer edge exists only for a point Sun.

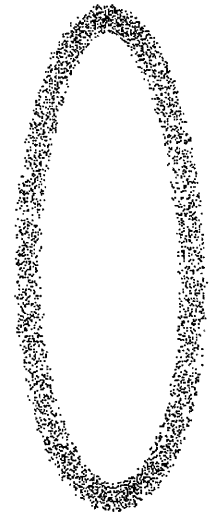

Fig. 13. Simulation of Bottlinger's ring for gyrating crystals with tilt $\psi = 2°$. The width of the ring is equal to the Sun's diameter (0.5°). Note that no subsun is present.

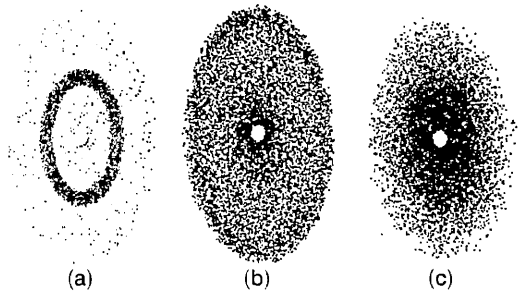

Fig. 14. Simulations of elliptical halos for $\phi = 55°$ and $\psi_{max} = 2°$ for a cloud of (a) 8000 horizontal crystals and 2000 gyrating crystals, (b) 10,000 gyrating crystals, (c) 10,000 swinging crystals. Note that gyrating crystals do not produce a ring.

The most striking elliptical halos are produced by hybrid clouds that consist of both gyrating and horizontal crystals. In this case, the ring is created by one reflection from a tilted crystal and is redirected without distortion by one reflection from a horizontal crystal. As only one tilted crystal produces this elliptical halo, its vertical angular diameter is four times the crystal tilt. The rays that strike two tilted crystals produce a much fainter outer ring with twice the diameter of the inner ring. We must point out, however, that this simple case does not match the observed ratio of angular diameters (1.6:1) in the one known case of multiple elliptical halos in Finland on 12 April 1993.

Radiative Transfer Effects

The simulations of elliptical halos shown in Fig. 14 employ the assumption that every light beam entering the cloud strikes either the top or the bottom of two perfectly reflecting plane crystals and then reaches the observer without loss. In fact, all halos are produced by imperfectly reflecting, solid crystals in clouds of finite optical thickness and are correspondingly less intense than idealized halos in perfect clouds. Furthermore, any halo produced by light striking two or more crystals will have still lower intensity, and it is natural to ask whether it can be seen. These considerations mandate that we include the crystal albedo and treat all halos as problems in radiative transfer.[30]

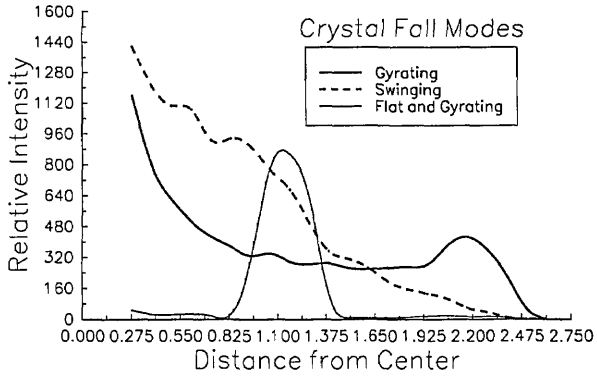

Fig. 15. Horizontal profiles of relative intensity for the elliptical halos of Fig. 14.

The light contributing to Bottlinger's rings and elliptical halos can be reflected from either the top or the bottom horizontal face of the crystal, but not from the vertical sides. The crystal albedo therefore depends on both the Fresnel reflection coefficients, which are functions of incidence angle, and on the crystal aspect ratio. Crystal albedo increases with increasing solar zenith angle and crystal aspect ratio and is therefore largest when the Sun is near the horizon and for thin plates and dendrites. Typical values of crystal albedo for a high Sun are less than 0.1, but can exceed 0.4 when $\phi > 80°$ and the aspect ratio exceeds 50. The effect of zenith angle and crystal aspect ratio on the intensity of Bottlinger's rings is shown in Fig. 16. The rings are far more intense when $\phi = 80°$ than when $\phi = 55°$ and are also more intense for an aspect ratio of 100 than for an aspect ratio of 5.

When the Sun is near the horizon, the intensity of the rings also contains marked vertical asymmetry because of the rapid increase of the Fresnel reflection coefficients as the incidence angle approaches 90°. The resulting asymmetry can be seen in both Plate 26 and in the vertical scan of Fig. 2, in which the top of the ring is much brighter than the bottom. Figure 17 compares vertical intensity profiles through the center of two of the Bottlinger rings in Fig. 16. The scan through the ring at $\phi = 55°$ shows almost no asymmetry, but the top of the ring at $\phi = 80°$ is almost twice as bright as the bottom. The pronounced maximum intensity in the center of the simulations is probably missing from Fig. 2 because the film was overexposed.

The effect of cloud optical thickness on halo brightness produced by either one or two reflections is described by the cloud model shown in Fig. 18. The vertical coordinate z increases downward from 0 at cloud top to h at cloud base. The cloud has scattering cross section σ and effective optical thickness $\tau_{eff} = \sigma h \sec(\phi)$. The halo beam that reaches the observer is considered to be a focused beam of reflected sunlight with zenith angle ϕ that suffers depletion from scattering as it passes through the cloud. The small change in zenith angle of the beam

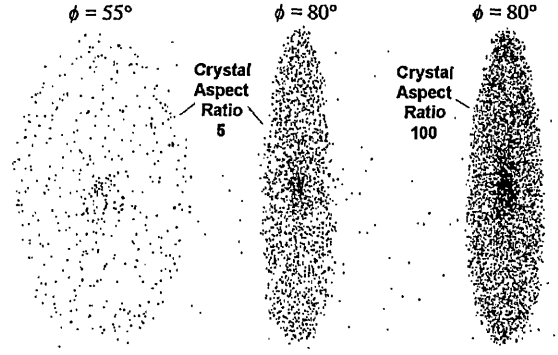

Fig. 16. Simulations of relative intensity of Bottlinger's rings for $\psi_{max} = 3°$ that show the effect of solar zenith angle ϕ and crystal aspect ratios. Note that the brightest ring occurs when both ϕ and the crystal aspect ratio are large.

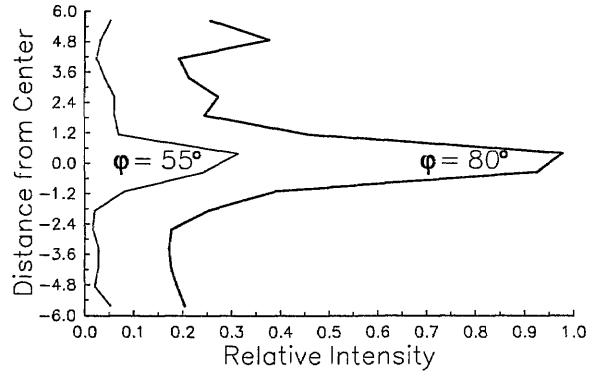

Fig. 17. Vertical profiles of relative intensity for Bottlinger's rings with $\psi_{max} = 3°$ for the case in which $\phi = 80°$ and crystal aspect ratio = 100 and the case in which $\phi = 55°$ and crystal aspect ratio = 5. Note that when $\phi = 80°$ the top of the ring is brighter than the bottom.

that is due to striking a slightly tilted crystal is included in the numerical model but is neglected in the theory presented below because it greatly complicates the mathematics and has only a minimal impact on the intensity of the light beam except quite near the horizon, where the plane-parallel assumption is invalid.

The probability that light will reach a crystal at depth z_1 in the cloud without being scattered is

$$\frac{B_{0\downarrow}(z_1)}{B_0} = \exp[-\sigma z_1 \sec(\phi)],$$

so that the fraction of the beam penetrating the cloud without suffering any scattering is

$$\frac{B_{0\downarrow}(h)}{B_0} = \exp(-\tau_{\text{eff}}).$$

The elemental contribution of light reflected from the first crystal at height z_1 and elemental volume $\sec(\phi)dz_1$ is

$$dB_{1\uparrow}(z_1) = \sigma \sec(\phi) B_{0\downarrow}(z_1) dz_1.$$

The light that reaches height z_2 from all crystals $z_1 > z_2$ is

$$B_{1\uparrow}(z_2) = \int_{z_2}^{h} dB(z_1)\exp[-\sigma(z_1 - z_2)\sec(\phi)]$$

$$= \frac{B_0}{2}\{\exp[-\sigma z_2 \sec(\phi)] - \exp[\sigma(z_2 - 2h)\sec\phi]\}.$$

The relative intensity of a light beam that emerges from the top of the cloud after a single reflection is therefore

$$\frac{B_{1\uparrow}(0)}{B_0} = \frac{1}{2}[1 - \exp(-2\tau_{\text{eff}})].$$

This is the beam that produces the subsun and Bottlinger's rings. The relative brightness, shown in Fig. 19, increases monotonically with increasing cloud optical thickness to a large value of 0.5, which is why rainbows and halos seen from above clouds often appear so bright. Nevertheless, the most spectacular rings should be seen for $\tau_{\text{eff}} \approx 1$ because multiple scattering reduces the contrast of the rings for optically thick clouds by disproportionately brightening the background.

Some of the light that is reflected upward within the cloud may strike a second crystal and be redirected downward to produce elliptical halos. The probability that a light beam will exit the bottom of the cloud after reflecting from two crystals is

$$\frac{B_{2\downarrow}(h)}{B_0} = \frac{1}{4}\exp(-\tau_{\text{eff}})[2\tau_{\text{eff}} - 1 + \exp(-2\tau_{\text{eff}})].$$

$B_{2\downarrow}$ attains a maximum at an effective optical depth, $\tau \sec(\phi) \approx 1.3$. Much thinner clouds have too few

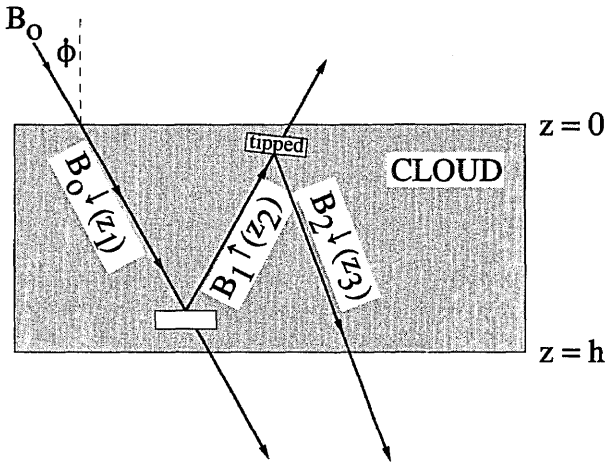

Fig. 18. Plane parallel cloud with sunlight B_0 shining on it from zenith angle, ϕ. Light passing downward through the cloud is $B_{0\downarrow}$, light scattered upward is $B_{1\uparrow}$, and light scattered back downward a second time is $B_{2\downarrow}$.

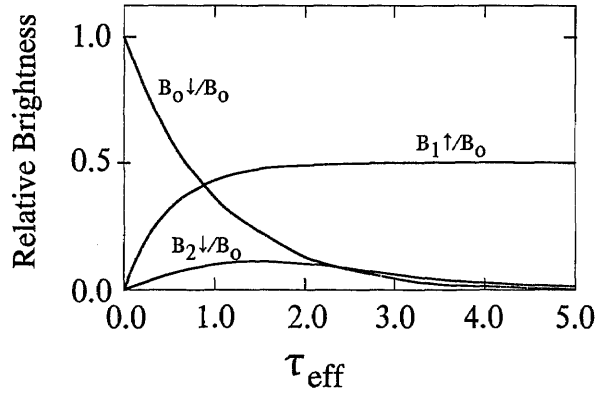

Fig. 19. Solutions for $B_{0\downarrow}/B_0$, $B_{1\uparrow}/B_0$, and $B_{2\downarrow}/B_0$ versus effective cloud optical thickness for a cloud of perfectly reflecting crystals.

crystals to produce a bright elliptical halo, whereas optically thick clouds invariably scatter light several times before it passes through the cloud. The maximum value of $B_{2\downarrow}/B_0$ for perfectly reflecting thin crystals is approximately 0.1, which compares with a maximum value of somewhat less than 1.0 for most refraction halos.[30] Thus, even when two reflections from an ice crystal with realistic albedos are included, distinct elliptical halos should be plainly visible in clean air so long as enough crystals have the proper fall mode.

Summary and Conclusions

In this paper we presented Monte Carlo simulations of subsuns, Bottlinger's rings, and elliptical halos in an attempt to explain their major features. Subsuns are circular or vertically elongated spots of light seen at the Sun's specular reflection point when one is flying above ice crystal clouds. Bottlinger's rings are rare, almost elliptical rings that form around subsuns. Rarest of all are the elliptical halos, which form around the Sun and have a vertical angular diameter of 6° or more. All three phenomena are elongated vertically and have an eccentricity that increases as the Sun nears the horizon.

All these phenomena are colorless, so we assumed that they are produced by sunlight that is reflected from ice crystals that either fall horizontally, undergo pendulum oscillations of tilt, or gyrate with constant tilt. One main problem we addressed was to find the crystal fall mode that correctly matches the observed brightness distributions.

The simulations confirm the established idea that subsuns are produced by reflection of sunlight from either horizontal or swinging ice crystals. The mechanism that produces the rare Bottlinger's rings is more controversial. Density scans of four cases show that only one has a distinct brightness minimum between the ring and the subsun, whereas in the three other cases brightness decreases monotonically outward. Thus the eye exaggerates the impression of a bright ring that is due to a Mach-band effect. A cloud of swinging crystals with identical maximum tilt angles produces a bright ring only for large crystal tilts and high Sun elevation angles. Only gyrating crystals produce a sharp ring surrounding a much darker sky, but, as gyrating crystals do not produce a subsun, such a cloud must also contain some horizontal crystals as well. Similar hybrid clouds have successfully been invoked to explain halo complexes and are a natural consequence of a distribution of ice-crystal sizes.

We hypothesized that elliptical halos surrounding the Sun or the Moon are produced by two reflections from nearly horizontal ice-crystal surfaces. Simulations showed that a cloud that consists of swinging crystals produces only an aureole, whereas a cloud of gyrating crystals can produce a somewhat brighter ring at the periphery of a disk. Only a cloud that consists of both gyrating and horizontal crystals produces a distinct bright ring surrounding a much darker sky. Such a cloud can also produce a second, much duller ring with twice the angular radius.

We noted both the strong and the weak points of our hypothesis that elliptical halos are produced by two reflections. Almost all elliptical halos are white, which bespeaks reflection. A preliminary meteorological analysis for three cases of elliptical halos indicates that each occurred in low clouds at −15 °C. Only large ice crystals fall in a tilted mode, whereas dendrites and stellars produced at high supersaturations near −15 °C tend to be the largest single crystals. Such multifaceted crystals reflect light well but do not produce coherent refraction halos. This is consistent with the observation that most elliptical halos are not accompanied by other halo phenomena. One troubling discrepancy between theory and observation is that even though the vertical elongation of the elliptical halos does increase with increasing solar zenith angle, it differs substantially from the theoretical shape caused by reflection. Another problem involves the case of three concentric rings, for which none of the rings has twice the angular radius of the others, and which we cannot explain.

We conclude that we have found the principal mechanism responsible for Bottlinger's rings and for elliptical halos, but acknowledge that enough tantalizing discrepancies exist between the theory and the few observations and reports to warrant continued attention to these rare atmospheric gems.

We thank Mike Fiorino and Fred Mertz for the use of their photographs, and Pekka Parviainen, Jukka Ruoskanen, and Marko Riikonen for the invaluable data on and descriptions of the elliptical halos. We also thank J. Shanks for useful discussions about subsuns and Gunther Können for useful guiding comments regarding Bottlinger's rings. Walter Tape's incisive and informative review goaded us into markedly improving the quality of the paper. Some of the calculations were performed on computers purchased by Gedzelman through National Science Foundation grants 8950473 and ATM 9106474.

Appendix A. Reflection Geometry

The geometry of reflection by an arbitrarily oriented surface can be described vectorially (Fig. 20). Unit vectors I and N, which represent the incident and the normal vectors, respectively, were used to solve for **R**,

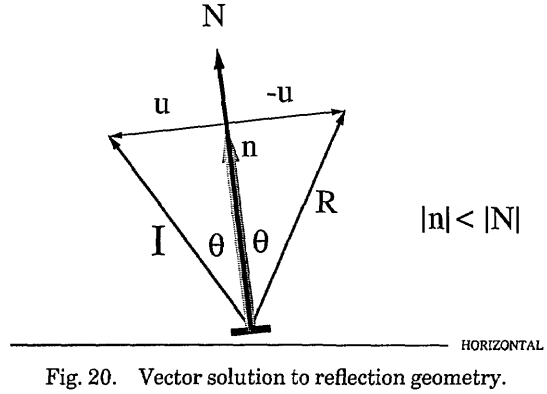

Fig. 20. Vector solution to reflection geometry.

the reflected ray. The vectors $\mathbf{n} = I \cos i$ and $\mathbf{u}$ were defined such that $I = \mathbf{n} + \mathbf{u}$. The law of reflection requires that $\mathbf{R} = \mathbf{n} - \mathbf{u}$. Once $\mathbf{R}$ was in hand, it was then projected onto the observer's plane, which is perpendicular to $\mathbf{R}(\beta = 0)$.

References

1. J. M. Pertner and F. M. Exner, *Meteorologische Optik* (Wilhelm Braumuller, Vienna, 1922), 397–398.
2. K. D. Rockwitz, "Scattering properties of horizontally oriented ice crystal columns in cirrus clouds. Part 1," Appl. Opt. **28,** 4103 (1989).
3. D. K. Lynch, and F. C. Mertz, "Bottlinger's rings," in *Light and Color in the Open Air,* Vol. 13 of OSA 1993 Technical Digest Series (Optical Society of America, Washington, D.C., 1993), pp. 73–77.
4. R. G. Greenler, A. J. Mallmann, M. Drinkwine, and G. Blumenthal, "The origin of Sun pillars," Am. Sci. **60,** 292–302 (1972).
5. J. G. Shanks, F. C. Mertz, C. B. Blasband, and T. Kassal, "Specular scattering from cirrus clouds: a first-order model," in *Proceedings of the Cloud Impact on Department of Defense Operations and Systems 1991,* D. Grantham and W. Snow, eds. (U.S. Government Printing Office, Washington, D.C., 1991), p. 207.
6. C. F. Bottlinger, "An interesting phenomenon seen during a balloon trip," Meteorol. Z. **25,** 74 (1910).
7. K. Stuchtey, "Untersonnen und Lichtsäulen an Sonne und Mond," Ann. Phys. (Leipzig) **59,** 33–55 (1919).
8. R. S. Scorer, *Clouds of the World* (Stackpole, Harrisburg, Pa., 1972), pp. 146–147. The photograph of Bottlinger's rings appears in Plate 13.3.11.
9. Photographs shown here are provided by A. B. Fraser, M. Fiorino, and F. C. Mertz.
10. C. M. Broomall, "Lunar halo," Science **13,** 549 (1901).
11. F. Schlesinger, "Elliptical lunar halos," Nature (London) **91,** 110–111, (1913).
12. R. G. Greenler, *Rainbows, Halos and Glories* (Cambridge U. Press, Cambridge, 1980).
13. J. Hakumaki, and M. Pekkola, "Rare vertically elliptical halos," Weather **44,** 466–473 (1989).
14. M. Pekkola, "Arvoituksellinen Hissikin halo," Tahdet ja Avaruus **18,** 60–63 (1988).
15. M. Pekkola, "Finnish Halo Observing Network: Search for rare halo phenomena," Appl. Opt. **30,** 3542–3544 (1991).
16. M. Riikonen and J. Ruoskanen, "Observations of vertically elliptical halos," Appl. Opt. **33,** 4537–4538 (1994).
17. P. Parviainen, V. Mäkelä, M. Pekkola, and C. B. Bohren, "Vertical elliptical coronas," *Light and Color in the Open Air,* Vol. 13 of 1993 OSA Technical Digest Series (Optical Society of America, Washington, D.C., 1993), pp. 73–77.
18. F. Ratliff, *Mach Bands: Quantitative Studies on Neural Networks in the Retina* (Holden-Day, New York, 1965).
19. T. N. Cornsweet, *Visual Perception* (Academic, New York, 1970).
20. The optical properties of light undergoing specular reflection from a horizontal surface of rippled water were originally studied, in order to understand sea glitter, by E. O. Hulburt, "The polarization of light at sea," J. Opt. Soc. Am. **24,** 35–42 (1943). See also C. Cox and W. Munk, "Measurement of the roughness of the sea surface from photographs of the Sun's glitter," J. Opt. Soc. Am. **44,** 838–850 (1954). Since that time, a modest body of literature has grown around the subject, the most notable being the work of Longuet-Higgins [see, e.g., M. S. Longuet-Higgins, "Reflection and refraction at a random moving surface. I. Pattern and paths of specular points," J. Opt. Soc. Am. **50,** 838–844 (1960); "Reflection and refraction at a random moving surface. II. Number of specular points in a Gaussian surface," J. Opt. Soc. Am. **50,** 845–850 (1960); "Reflection and refraction at a random moving surface. III. Frequency of twinkling in a Guassian surface," J. Opt. Soc. Am. **50,** 851–856 (1960).
21. W. W. Wilmarth, N. E. Hawk, and R. L. Harvey, "Steady and unsteady motions and wakes of freely falling disks," Phys. Fluids. **7,** 197–208 (1964).
22. G. E. Stringham, D. B. Simons, and H. P. Guy, "The behavior of large particles falling in quiescent liquids," U.S. Geological Survey prof. paper 562-C (U.S. Geological Survey, Washington, D.C., 1969).
23. R. List and R. S. Schemenauer, "Free-fall behavior of planar snow crystals, conical graupel and small hail," J. Atmos. Sci. **28,** 110–115 (1971).
24. H. R. Cho, J. V. Iribane, and W. G. Richards, "On the orientation of ice crystals in a cumulonimbus cloud," J. Atmos. Sci. **38,** 1111–1114 (1981).
25. K. O. L. F. Jayaweera and R. E. Cottis, "Fall velocities of plate-like and columnar ice crystals," Q. J. R. Meteorol. Soc. **95,** 703–709 (1969).
26. A. H. Auer and D. L. Veal, "The dimensions of ice crystals in natural clouds," J. Atmos. Sci. **27,** 919–926 (1970).
27. R. E. Stewart and R. List, "Gyrational motion of disks during free-fall," Phys. Fluids **26,** 920–927 (1983).
28. H. R. Pruppacher and J. D. Klett, *Microphysics of Clouds and Precipitation,* (Reidel, Dordrecht, The Netherlands, 1978), pp. 38–39.
29. S. D. Gedzelman, "Simulating rainbows and halos in color," Appl. Opt. **33,** 4607–4613 (1994).
30. S. D. Gedzelman, "Visibility of halos and rainbows," Appl. Opt. **19,** 3068–3074 (1980).